

Light Element Depletion in Contracting Brown Dwarfs and Pre–Main-Sequence Stars

Greg Ushomirsky, Christopher D. Matzner, Edward F. Brown, Lars Bildsten, Vadim G. Hilliard
and Peter C. Schroeder¹

Department of Physics and Department of Astronomy
601 Campbell Hall
University of California, Berkeley, CA 94720

Accepted to ApJ

ABSTRACT

We present an analytic calculation of the thermonuclear depletion of the light elements lithium, beryllium, and boron in fully convective, low-mass stars. Under the presumption that the pre–main-sequence star is always fully mixed during contraction, we find that the burning of these rare light elements can be computed analytically, even when the star is degenerate. Using the effective temperature as a free parameter, we constrain the properties of low-mass stars from observational data, independently of the uncertainties associated with modeling their atmospheres and convection. Our results are in excellent agreement with the detailed calculations of D’Antona & Mazzitelli (1994) and Chabrier, Baraffe, & Plez (1996). Our analytic solution explains the dependence of the age at a given level of elemental depletion on the stellar effective temperature, nuclear cross sections, and chemical composition. These results are also useful as benchmarks to those constructing full stellar models. Most importantly, our results allow observers to translate lithium non-detections in young cluster members into a model-independent minimum age for that cluster. Using this procedure, we have found lower limits to the ages of the Pleiades (100 Myr) and Alpha Persei (60 Myr) clusters. Dating an open cluster using low-mass stars is also independent of techniques that fit upper main-sequence evolution. Comparison of these methods provides crucial information on the amount of convective overshooting (or rotationally induced mixing) that occurs during core hydrogen burning in the 5–10 M_{\odot} stars typically at the main-sequence turnoff for these clusters. We also discuss beryllium depletion in pre–main-sequence stars. Recent experimental work on the low energy resonance in the $^{10}\text{B}(p, \alpha)^7\text{Be}$ reaction has greatly enhanced estimates of the destruction rate of ^{10}B , making it possible for stars with $M \gtrsim 0.1M_{\odot}$ to deplete both ^{10}B and ^{11}B before reaching the main sequence. Moreover, there is an interesting range of masses, $0.085M_{\odot} \lesssim M \lesssim 0.13M_{\odot}$, where boron depletion occurs on the main sequence in less than a Hubble time, providing a potential “clock” for dating low-mass stars.

¹Currently at Space Sciences Laboratory, University of California, Berkeley, CA 94720

Subject headings: open clusters and associations — stars: abundances — stars: evolution — stars: fundamental parameters — stars: low-mass, brown dwarfs — stars: pre-main-sequence

1. Introduction

Due to low Coulomb barriers and purely strong-interaction reactions, most stars are able to destroy deuterium, lithium, beryllium, and boron via proton capture prior to reaching the main sequence. For low-mass stars ($M \lesssim 0.5 M_\odot$; the exact mass cutoff depends on the element, see § 2.2), light element depletion occurs while the star is fully convective (i.e., before the stellar core becomes radiative) and still contracting towards the main sequence. In fully convective stars, light elements are depleted throughout the star, and the photospheric abundance is a reliable indicator of the interior abundance. In the case of lithium, the depletion at the photosphere in these stars is readily observable. Deuterium is depleted on a contraction timescale when the central temperature is $T_c \approx (8\text{--}10) \times 10^5$ K, in which case the energy released from consuming all the deuterium ($D/H \approx 1.6 \times 10^{-5}$ in the local ISM, Piskunov et al. 1997) is comparable to the thermal energy content in the star. This slows contraction and nearly leads to a “deuterium main sequence” (Grossman & Graboske 1971, 1973; D’Antona & Mazzitelli 1985) at an age of order 1 Myr. For some masses, the deuterium burning occurs while the star is still accreting (Stahler 1988a). Once accretion and deuterium burning are complete (after 1–10 Myr, depending on the mass, Stahler 1988a) the star undergoes traditional Hayashi contraction. It is during this phase that lithium, beryllium, and boron are destroyed in most low-mass stars.

There has been much previous work on light element depletion in gravitationally contracting pre-main-sequence stars (Hayashi & Nakano 1963; Weymann & Moore 1963; Ezer & Cameron 1963; Bodenheimer 1965, 1966; Nelson, Rappaport, & Chiang 1993; D’Antona & Mazzitelli 1994 [hereafter DM94]; Chabrier, Baraffe, & Plez 1996 [hereafter CBP96]; Chabrier & Baraffe 1997 [hereafter CB97]). Motivated by lithium observations along the main sequence in open clusters (see Soderblom 1995 and Martín 1998 for recent reviews), many have calculated lithium depletion for stars of $M \gtrsim 0.5 M_\odot$ both during and after the pre-main-sequence phase (Vauclair et al. 1978; D’Antona & Mazzitelli 1984; Proffitt & Michaud 1989; Vandenberg & Poll 1989; Swenson, Stringfellow, & Faulkner 1990; Deliyannis, Demarque, & Kawaler 1990; Forestini 1994; Martín & Claret 1996). For stars with $M \gtrsim 0.5 M_\odot$, most of the lithium burns after convection has halted in the stellar core. Accurate predictions of lithium depletion then depend on the temperature at the bottom of the retreating convective zone. The location of the convective/radiative boundary and the amount of mixing across it depend on opacity, treatment of convection, and rotation; proper handling of these effects remains an open question. The range of observational results on lithium depletion in young clusters also points to these effects playing an important role for $M \gtrsim 0.5 M_\odot$ (Martín 1998).

In this paper, we analytically calculate the depletion of lithium, beryllium, and boron for those stars that are always fully convective during depletion. The interstellar abundances of these elements is low enough that the energy released by their fusion cannot halt (nor appreciably slow) stellar contraction. Efficient convection throughout the star allows us to represent it accurately as a fully mixed $n = 3/2$ polytrope, for which analytic treatment of element depletion is tractable (Bildsten et al. 1997, hereafter B²MU, also see Hayashi & Nakano 1963; Stevenson 1991; Burrows & Liebert 1993). Our analytic calculation gives a convenient formula for the time and central temperature at which elemental depletion occurs, as well as its dependence on stellar parameters, such as the mass and composition of the star. Most importantly, our treatment allows us to survey the effects of the presently most uncertain aspect of stellar modeling, the effective temperature T_{eff} (which sensitively depends on the treatment of the photospheric boundary conditions, opacities, and the treatment of convection). These uncertainties have motivated a number of calculations (Pozio 1991; Magazzù, Martín, & Rebolo 1993; Nelson, Rappaport, & Chiang 1993; DM94; CBP96; CB97), each employing different treatments of these uncertain factors. We show that for a given T_{eff} and M we can reproduce the results of these prior works to high accuracy. Moreover, our approach allows the inferred effective temperature of an observed star to be used directly in analyzing light element depletion observations, without first placing it on a theoretical evolutionary track.

A previous application of our theoretical results to low-mass stars in the Pleiades (B²MU) confirmed in a model-independent way the 100 Myr minimum age originally determined from lithium observations by Basri et al. (1996). As we discuss in §5.1.2, applying our method to the lithium non-detections in pre-main-sequence stars in the open cluster Alpha Persei (Zapatero Osorio et al. 1996) yields a minimum age of 60 Myr for that cluster, independently of the effective temperature scale for low-mass stars. We stress that lithium observations of contracting pre-main-sequence stars in young open clusters provide accurate and reliable minimum ages. This is very important, because for the age range (10–200 Myr) when low-mass stars ($0.09 \lesssim M/M_{\odot} \lesssim 0.4$) are actively depleting lithium, stars with masses of 4–15 M_{\odot} are leaving the main sequence (using Maeder & Meynet’s 1989 $t_{\text{MS}}(M)$ relations with overshoot of 1/4 of the pressure scale height at the convective/radiative boundary). Confirming or denying that these stars live longer on the main sequence due to enhanced mixing (from convective overshoot) is a crucial issue. White dwarfs have also been found in many of these young clusters and extrapolating backwards in time from the cooling age allows one to estimate the mass of the progenitor star. This extrapolation depends critically on the presumed age of the cluster (see Reid 1996 for an up-to-date discussion).

We begin in § 2 by justifying the treatment of the contracting star as an $n = 3/2$, fully mixed polytrope. We also outline two important limitations to our approach, the formation of a radiative core and the onset of substantial hydrogen burning. Our analytic calculation of hydrogen burning also yields a convenient fitting formula for the stellar radius and surface gravity as a function of T_{eff} along the zero-age main sequence (summarized in Appendix A). In § 3, we update the proton capture rates for the light elements and discuss the possible effects of a sub-threshold resonance in proton captures on beryllium. Section 4 presents the equation describing light element depletion,

our treatment of the correction due to electron degeneracy at the time of depletion, and our method for solving the resulting equations. In § 5, we provide detailed fitting formulae for the depletion of different light elements and compare our results to previous numerical work. We emphasize that our technique makes robust predictions, even when the instantaneous depletion time is much less than the contraction time. This is important, since lithium is detectable even when substantially depleted. We also apply our results to lithium observations in open clusters. We conclude in § 6 with a brief summary and a few speculations.

2. The Internal Structure of Pre–Main-Sequence Stars

Detailed numerical evolutionary calculations of contracting pre–main-sequence (and pre–brown-dwarf) stars have been carried out by a number of authors (see Burrows & Liebert 1993 for a review). As shown by Nelson, Rappaport, & Joss (1986), very low-mass stars ($M \lesssim 0.03M_{\odot}$) remain completely and efficiently convective even at ages of about 4.5 Gyr. Higher-mass stars ($M \gtrsim 0.07M_{\odot}$) stop convecting only once they are degenerate enough (and, likewise, cool enough) for electron conduction to carry the necessary flux; this takes at least 5 Gyr (Stevenson 1991). Of those that burn hydrogen, stars of mass $M \lesssim 0.3M_{\odot}$ remain fully convective even after they settle onto the main sequence, while stars of mass $M \lesssim 0.5M_{\odot}$ remain fully convective at least until the end of ${}^7\text{Li}$ burning (DM94). This critical mass is lower for beryllium and boron burning. As long as we restrict our attention to masses below this critical value (derived in § 2.2), full and efficient convection prevails during the period of light element depletion.

The effective temperature of a fully convective star determines the contraction rate and is found by matching the entropy in the deep interior to that below the photosphere (see Stahler 1988b for an excellent review of Hayashi contraction). For these low-mass stars with $T_{\text{eff}} \lesssim 4000$ K, the opacities are still uncertain, and the treatment of convection near the photosphere is still open to debate. The differing input physics results in different effective temperatures for the same stellar mass. For example, DM94 found that for a $0.2M_{\odot}$ star, T_{eff} ranges from 3350 K to 3640 K depending on whether Alexander et al. (1989) or Kurucz (1991) opacities were used in the stellar envelope. On the other hand, for the same star, CB97 get $T_{\text{eff}} = 3250$ K using Alexander & Ferguson (1994) opacities, a non-gray atmosphere (Allard & Hauschildt 1997), and a more consistent treatment of convection near the photosphere, as opposed to a gray atmosphere used by DM94. In addition, the uncertainty in the effective temperature inferred from the observed spectrum can be as large as ± 125 K (Kirkpatrick et al. 1993), and discrepancies between effective temperature scales from different authors can be much higher, up to 500 K (Martín, Rebolo, & Magazzù 1994; Zapatero Osorio et al. 1996).

Despite the variations in the exact value of T_{eff} that stem from differences in the input physics, most calculations do agree that T_{eff} *remains approximately constant during the fully convective contraction phase*. Thus, rather than rely on a particular choice of input physics to fix $T_{\text{eff}}(M, R)$, we choose to view it as a free parameter that is constant during fully convective contraction, and

explore its effect on elemental depletion in a model-independent way.

2.1. Fully Convective Stars

In a fully (i.e., core to photosphere; see below for a caveat) and efficiently convecting star the entropy per unit mass is independent of position within the star and decreases as the star contracts. This is true even if the star is partially degenerate. The entropy of a gas comprised of nondegenerate ions of mean molecular weight $\mu_i \equiv \rho N_A/n_i$ and electrons with weight μ_e is

$$s = \text{const} - \frac{k_B N_A}{\mu_i} \ln F_{1/2}(\eta) + \frac{k_B N_A}{\mu_e} \left(\frac{5}{3} \frac{F_{3/2}(\eta)}{F_{1/2}(\eta)} - \eta \right), \quad (1)$$

where the constant term (which contains the entropy of mixing) depends only on the composition, η is the degeneracy parameter (ratio of the electron chemical potential to $k_B T$), $F_n(\eta)$ is the n th-order Fermi-Dirac function

$$F_n(\eta) = \int_0^\infty \frac{x^n dx}{1 + \exp(x - \eta)}, \quad (2)$$

and $F_{1/2}(\eta) \propto \rho/\mu_e T^{3/2}$ (see, for example, Clayton 1983). The entropy is a monotonic function of the degeneracy parameter, so for constant μ_e and μ_i equation (1) is invertible, $\eta = \eta(s)$. Therefore, in an isentropic star the degree of electron degeneracy is constant (Stevenson 1991; Burrows & Liebert 1993; B²MU). The equation of state is

$$P = \frac{\rho N_A}{\mu_{\text{eff}}} k_B T, \quad (3)$$

where

$$\frac{1}{\mu_{\text{eff}}} \equiv \left(\frac{1}{\mu_i} + \frac{1}{\mu_e} \frac{2}{3} \frac{F_{3/2}(\eta)}{F_{1/2}(\eta)} \right) \approx \left(\frac{1}{\mu_i} + \frac{1}{\mu_e} \frac{(1 + 0.1938 F_{1/2}(\eta))^{5/3}}{1 + 0.12398 F_{1/2}(\eta)} \right). \quad (4)$$

The approximation used in the second equality is from Larson and Demarque (1964) and is accurate to within 0.02% for $\eta < 30$. In essence, for a given pressure and density, the temperature is reduced by a degeneracy dependent factor that is constant along an adiabat. This means that the adiabatic exponents are $\Gamma_1 = \Gamma_2 = \Gamma_3 = 5/3$, and the star is described by an $n = 3/2$ polytrope regardless of the degree of electron degeneracy (Hayashi & Nakano 1963; Stevenson 1991; Burrows & Liebert 1993; B²MU). Moreover, μ_{eff} is constant throughout the star. Accordingly, we have $T = T_c \Theta(\xi)$ and $\rho = \rho_c \Theta^{3/2}(\xi)$, where $\xi \equiv \xi_1 r/R$ is the radial coordinate, and $\Theta(\xi)$ is the Lane-Emden function for $n = 3/2$, which crosses zero at $\xi_1 = 3.65$. The central density and temperature are

$$\rho_c = 8.44 \left(\frac{M}{M_\odot} \right) \left(\frac{R_\odot}{R} \right)^3 \text{ g cm}^{-3}, \quad (5)$$

$$T_c = 7.41 \times 10^6 \left(\frac{\mu_{\text{eff}}}{0.6} \right) \left(\frac{M}{M_\odot} \right) \left(\frac{R_\odot}{R} \right) \text{ K}. \quad (6)$$

In the non-degenerate limit $1/\mu_{\text{eff}} \rightarrow 1/\mu_i + 1/\mu_e \equiv 1/\mu$, and the stellar model is completely specified. For an arbitrary degree of degeneracy, however, the stellar radius, R , and μ_{eff} are related by

$$\frac{R}{R_{\odot}} = \frac{7.73 \times 10^{-2}}{\mu_{\text{eff}} \mu_e^{2/3} F_{1/2}^{2/3}(\eta)} \left(\frac{M_{\odot}}{M} \right)^{1/3}. \quad (7)$$

We will use this relation in § 4 to calculate the depletion.

In the above discussion we assumed that efficient convection assures that the star is isentropic throughout, and the entire star is well-described by an $n = 3/2$ polytrope. Electron degeneracy alone cannot modify the polytropic structure to affect this relation. However, near the photosphere, the entropy cannot be constant for two reasons. First, near the photosphere and above it, radiative transport must carry most of the energy flux, and hence the entropy in such regions must increase outwards. Moreover, immediately below the photosphere, and especially in the hydrogen ionization zone, convection tends to be inefficient and superadiabatic, leading to a decrease of entropy with radius; see Figure 3 of Stahler (1988b) for an illustration of this behavior. Therefore, the relation between the entropy in the interior and that at the photosphere is not trivial. A significant fraction of the effort in numerically simulating pre-main-sequence evolution is aimed at disentangling this relationship in order to self-consistently calculate the effective temperatures for these stars.

The effect of these complications on the stellar radius is extremely small. The radiative skin in the stars under consideration is tremendously thin, $\Delta R/R < 10^{-4}$, $\Delta M \sim 10^{-10} M_{\odot}$ (Burrows, Hubbard, & Lunine 1989). Similarly, the ratio of the temperature at the ionization zone ($T_{\text{ioniz}} \sim 10^4$ K) to the central temperature ($T_c \sim 10^6$ K) is of order 10^{-2} ; the virial theorem then implies that the ionization zone is located in the outer 1% of the stellar radius. Moreover, the ratio of the pressure at the ionization zone to the central value is $P_{\text{ioniz}}/P_c = (T_{\text{ioniz}}/T_c)^{5/2}$. Since the envelope is geometrically thin, the pressure at the ionization zone is $P_{\text{ioniz}} \approx GM\Delta M/4\pi R^4$, while the pressure at the center of an $n = 3/2$ polytrope is $P_c = 9.7GM^2/4\pi R^4$, so the mass of neutral gas in the star is just $\Delta M \sim 10^{-4}M$. Thus, most of the mass (and volume) of the star is fully ionized, as well as fully (i.e., core to photosphere) and efficiently convective, and the stellar structure is well-described by an $n = 3/2$ polytrope until radiative heat transport at the stellar center (§ 2.2) or Coulomb corrections (§ 5.1.1) become important. The difference between the true radius of the star and that given by equations (5) – (7) is extremely small, and we are justified in neglecting it.

Except during deuterium burning, the energy output from burning light elements is insufficient to halt the gravitational contraction (however, see §2.2 for discussion of effects of hydrogen burning). Thus, we assume that the luminosity of the star, L , is balanced by energy generation due to gravitational contraction alone. For an $n = 3/2$ polytrope, a virial analysis gives

$$L = 4\pi R^2 \sigma_{\text{SB}} T_{\text{eff}}^4 = -\frac{3}{7} \frac{GM^2}{R^2} \frac{dR}{dt}; \quad (8)$$

this relation holds even if the star is partially or strongly degenerate. As discussed in § 2, we assume that T_{eff} is constant during contraction. The time $t = 0$ then corresponds to the onset of

quasistatic contraction, which we approximate with a nonphysical initial state of infinite radius and contraction rate. Therefore t differs from the chronological age because of the deuterium burning phase, the initial radius on the theoretical stellar birthline (Stahler 1988a), and changes in the effective temperature during contraction. However, as long as the effective temperature is correct when the depletions occur, t will not differ significantly from the chronological age. Integrating equation (8), we obtain the stellar radius as a function of time,

$$\frac{R}{R_\odot} = \frac{17.1}{T_{e3}^{4/3} t_6^{1/3}} \left(\frac{M}{M_\odot} \right)^{2/3}, \quad (9)$$

where $T_{e3} \equiv T_{\text{eff}}/1000 \text{ K}$ and $t_6 \equiv t/10^6 \text{ yr}$. Since the radius of the star is completely determined by $F_{1/2}(\eta)$, we combine the above relation with equation (7) to obtain a transcendental equation,

$$\mu_{\text{eff}} F_{1/2}^{2/3}(\eta) = 4.53 \times 10^{-3} \left(\frac{M_\odot}{M} \right) \left(\frac{T_{e3}^4 t_6}{\mu_e^2} \right)^{1/3}, \quad (10)$$

for the degeneracy parameter as a function of time.

2.2. The Onset of Hydrogen Burning and the Formation of a Radiative Core

As the star approaches the main sequence, p-p reactions generate an increasing amount of energy. Eventually, the relation for the contraction rate (eq. [8]), which assumes that the energy generation is only due to gravitational contraction, ceases to hold. This condition defines the lower mass limit of our calculations' validity for beryllium and boron depletion during pre-main-sequence contraction. We calculate this limit by comparing the nuclear luminosity L_{nuc} (i.e., the total rate of energy generation due to p-p reactions in the star) to the energy release rate due to contraction (eq. [8]). Note that stars depleting lithium either burn it before p-p reactions become an important source of energy (however, see § 5.1.1), or are not massive enough to reach the main sequence.

The specific rate of heat production (Clayton 1983) for the reactions $p + p \rightarrow {}^2\text{H} + e^+ + \nu_e$ and ${}^2\text{H} + p \rightarrow {}^3\text{He} + \gamma$ is

$$\epsilon_{\text{pp}} = 1.23 \times 10^6 f_{\text{scr}} X^2 \rho T_6^{-2/3} \exp\left(-\frac{33.8}{T_6^{1/3}}\right) \text{ erg s}^{-1} \text{ g}^{-1}, \quad (11)$$

where $T_6 \equiv T/10^6 \text{ K}$, ρ is in cgs units, X is the hydrogen mass fraction, and f_{scr} is the screening correction factor (Salpeter & Van Horn 1969). Further energy release from the PPI chain will not occur until the abundance of ${}^3\text{He}$ has increased to its equilibrium value; the timescale for this is greater than 1 Gyr at temperatures $\sim 5 \times 10^6 \text{ K}$ (Clayton 1983). Since the reaction rate (eq. [11]) has such a steep temperature dependence, most burning occurs near the center of the star. Therefore, we can approximate the screening factor f_{scr} by its value at the stellar center. Moreover, if the star is fully convective, it is described by an $n = 3/2$ polytrope (see §2.1) regardless of the

extent of nuclear burning. Under these conditions, the nuclear luminosity is

$$L_{\text{nuc}} \equiv \int \epsilon_{\text{pp}} dm \approx 4.72 \times 10^{-2} T_{c6}^{0.36} \epsilon_{\text{pp}}(\rho_c, T_c) M, \quad (12)$$

where the prefactor in the above equation comes from integrating the reaction rate over an $n = 3/2$ polytrope and constructing a simple analytic fit to the result. Using equation (12), we have derived an analytic relation between the effective temperature along the zero-age main sequence and stellar radius and surface gravity (see Appendix A).

When the nuclear luminosity is much less than the luminosity due to gravitational contraction L_c (eq. [8]), the assumptions leading to the contraction law (eq. [9]) hold, and our depletion calculations are reliable. We indicate in Figures 1 and 2 the central temperatures and ages at which $L_{\text{nuc}} \approx 0.05L_c$ and $L_{\text{nuc}} \approx 0.50L_c$ (*heavy solid lines*). For comparison, we also show (*triangles*) a 1 Gyr isochrone (roughly, the main sequence) from CB97. Our results for light element depletion are only valid in the regions of the plots below the aforementioned lines. As one can see, lithium depletion is unaffected by the hydrogen burning, while the beryllium results are only valid for $M \gtrsim 0.1M_{\odot}$ (boron depletion will be discussed in § 5.3).

Although p-p reactions can slow the contraction rate, they do not alter the $n = 3/2$ polytropic stellar structure. However, for stars of mass $M \gtrsim 0.35M_{\odot}$ (Chabrier & Baraffe 1997) a radiative core forms during contraction. Formation of a radiative core breaks the polytropic structure, prevents mixing into the depletion region, and thus defines the upper mass limit of applicability of our depletion calculations. We estimate the central temperature at which convection ceases in the core as follows.

The gas at the stellar center is convectively unstable whenever the temperature gradient $d \ln T / d \ln P$ exceeds the adiabatic value $1 - 1/\Gamma_2$ (see, for example, Hansen & Kawaler 1994). In other words, the maximum rate of energy generation *at the center of the star* that can be balanced by radiative heat transport alone is

$$\epsilon_{\text{rad}} \equiv \left. \frac{\partial L(r)}{\partial m} \right|_{r=0} = \frac{64\pi}{3} \frac{G\sigma_{\text{SB}}}{\kappa} \frac{T_c^4}{P_c} \left(1 - \frac{1}{\Gamma_2} \right), \quad (13)$$

where κ is the opacity. The minimum rate of energy production ϵ_{rad} for which the stellar center is fully convective is just equation (13) with $\Gamma_2 = 5/3$. In pre-main sequence stars, the bulk of the energy is released by gravitational contraction, with the specific energy production rate

$$\epsilon_{\text{grav}} = -\frac{P}{\rho(\Gamma_3 - 1)} \frac{d}{dt} \ln \left(\frac{P}{\rho^{\Gamma_1}} \right) = -\frac{3}{2} \frac{k_B N_A T}{\mu_{\text{eff}}} \frac{d \ln R}{dt}; \quad (14)$$

the total luminosity L (equation [8]) is just the above rate integrated over the entire star. As the star approaches the main sequence, there is an additional small contribution ϵ_{pp} due to hydrogen burning (eq. [11]). We equate the total energy generation rate at the stellar center $\epsilon \equiv \epsilon_{\text{grav}} + \epsilon_{\text{pp}}$ with ϵ_{rad} and solve for T_c . We compute the opacity at the center from the OPAL tables (Rogers & Iglesias 1992) and use effective temperatures as a function of mass from CBP96 to compute

the contraction rate. The resulting radiative/convective boundary curves are plotted in Figures 1 and 2 (*heavy dot-dashed lines*). The stars develop radiative cores in the regions of the plots above the $\epsilon = \epsilon_{\text{rad}}$ curves. For ${}^7\text{Li}$, the mass, central temperature, and density at which half-depletion is coincident with the formation of a radiative core are $M_{1/2} \approx 0.5M_{\odot}$, $T_c \approx 4.1 \times 10^6$ K, and $\rho_c \approx 4.8 \text{ g cm}^{-3}$. This is in excellent agreement with CB97, who find that a radiative core forms in a $0.5M_{\odot}$ star at an age of 10^7 yr, when the lithium abundance is 0.52. The corresponding stellar parameters for which the formation of a radiative core is coincident with ${}^7\text{Li}$ depletion by a factor of 100 are $M_{1/100} \approx 0.44M_{\odot}$, $T_c \approx 4.3 \times 10^6$ K, and $\rho_c \approx 7.7 \text{ g cm}^{-3}$. For ${}^7\text{Li}$, our fully convective depletion calculations are therefore valid for $M \lesssim 0.45 - 0.5M_{\odot}$, depending on the desired depletion level.

We should point out that the above results are quite sensitive to the value of the opacity at the stellar center. If we write the opacity as $\kappa_{\circ} \rho^{\kappa_{\rho}} T^{\kappa_T}$ (with ρ and T in cgs units), we find that, at the central temperature where ${}^7\text{Li}$ is depleted by a factor of two, $\kappa_{\circ} = 5.66 \times 10^{21} \text{ cm}^2 \text{ g}^{-1}$, $\kappa_{\rho} = 0.347$, and $\kappa_T = -3.166$. The mass of the star that becomes radiative upon depleting half of its ${}^7\text{Li}$ content scales with κ_{\circ} and T_{eff} as $M_{1/2} \propto \kappa_{\circ}^{0.48} T_{\text{eff}}^{1.6}$. The sensitivity of observed lithium depletions to the interior opacity has previously been considered for higher mass main-sequence stars by Swenson et al. (1990) and Swenson et al. (1994), who adjusted the interior opacities by changing the metal content. Although they were considering stars of approximately solar mass, Swenson et al. (1990) found that an increase of 37% in the interior opacity increased the mass of a Hyades star at which the lithium was half-depleted by $\sim 20\%$, i.e., $M_{1/2} \propto \kappa_{\circ}^{0.5}$, similar to our estimated dependence.

3. Proton Capture Rates for Light Elements

We use thermonuclear reaction rates in the form

$$N_A \langle \sigma v \rangle = S f_{\text{scr}} T_6^{-j} \exp\left(-\frac{a}{T_6^{1/3}}\right) \text{ cm}^3 \text{ s}^{-1} \text{ g}^{-1}, \quad (15)$$

to approximate the rates of Caughlan & Fowler (1988, hereafter CF88). For non-resonant reactions $j = 2/3$, while for reactions affected by resonances the value of j has to be adjusted (see below). Here, S does *not* represent the astrophysical S-factor, but is rather, like a , a dimensionless parameter in the fit to the reaction rate. Table 1 shows the values of S and a found by fitting to the rates over the range of temperatures ($T_6 < 6$) appropriate for this work. Raimann (1993) recently incorporated new experimental results at low energies ($\approx 11\text{--}13$ keV) to update the rates for ${}^7\text{Li}$, adjusting the value of S from 6.4×10^{10} (CF88) to 7.2×10^{10} .

There are two stable boron isotopes with abundance ratios in the local ISM of ${}^{11}\text{B}/{}^{10}\text{B} = 3.4_{-0.6}^{+1.3}$ (Federman et al. 1996). The ${}^{10}\text{B}(p, \alpha){}^7\text{Be}$ reaction is resonant, as an excited state of the ${}^{11}\text{C}$ nucleus exists just 10 keV above the center-of-mass energy of the $p + {}^{10}\text{B}$ system. As a non-resonant reaction, the center-of-mass energy would be at $E_c = 3.46T_6^{2/3}$ keV, and the reaction occurs (as we show

later) at $T_6 \approx 6$, so that $E_c = 11.4 \text{ keV}$, and thus this resonance affects the cross section. Rauscher & Raimann (1996) recently corrected the CF88 rates for this broad resonance, which enhances the rate by at least a factor of 200 for the temperatures of interest. For $T_6 < 6$, a reasonable fit to the reaction rates that includes the resonance is to multiply the CF88 rates by $300(T_6/3)^{1/2}$. The entries for this reaction in Table 1 include the resonant correction.

There are potential problems with the ${}^9\text{Be}(p, \alpha){}^6\text{Li}$ rate as well, since an excited state of ${}^{10}\text{B}$ ($E_x = 6.56 \text{ MeV}$) lies just 25.7 keV below the energetic threshold. Current knowledge (see Ajzenberg-Selove 1988) holds that the angular momentum and parity of this state is either $J^\pi = 2^-$ or $J^\pi = 4^-$, with 4^- thought to be the better guess. The angular momentum and parity of ${}^9\text{Be}$ is $(3/2)^-$, while that of a proton is $(1/2)^+$. Hence, if this resonant state has $J^\pi = 4^-$, the proton must overcome a centrifugal barrier of angular momentum $\ell = 2$, and the resonant state will not contribute significantly to the reaction rate. But if instead $J^\pi = 2^-$, the resonance can proceed via s-wave ($\ell = 0$) and the rate will be greatly enhanced over the CF88 rate (Brown 1997).

To estimate the effect such a resonance would have, we parameterize the entrance channel by the dimensionless reduced width θ^2 (Clayton 1983). Crudely speaking, θ^2 measures the degree to which the compound $p + {}^9\text{Be}$ nucleus resembles the excited level of ${}^{10}\text{B}$. The cross section is then calculated using the Breit-Wigner formula (see Brown 1997 for details) with θ^2 as a free parameter. A good fit to the thermally-averaged rate for $J^\pi = 2^-$ (accurate to within 1% for $2 < T_6 < 5$) is

$$N_A \langle \sigma v \rangle \approx 3.53 \times 10^{16} \theta^2 T_6^{-1.367} \exp\left(-\frac{105.33}{T_6^{1/3}}\right) \text{ cm}^3 \text{ g}^{-1} \text{ s}^{-1}; \quad (16)$$

the total reaction rate is the sum of this equation and the standard non-resonant rate. For the temperatures of interest in low-mass stars, $T_6 \lesssim 6$, an s-wave resonance will dramatically boost the rates if $\theta^2 \gtrsim 0.01$. In this paper, in addition to using CF88 rates for ${}^9\text{Be}$, we use equation (16) to explore the effect of the resonance on beryllium depletion in pre-main-sequence stars.

4. The Depletion Equation

The central temperature needed for depletion can be roughly estimated as follows. Light elements are depleted when the nuclear destruction time at the center of the star,

$$t_{\text{dest}} \equiv \frac{1}{n_p \langle \sigma v \rangle} = 0.689 \left(\frac{M}{0.1 M_\odot}\right)^2 \left(\frac{\mu_{\text{eff}}}{0.6}\right)^3 \frac{T_{c6}^{j-3}}{S f_{\text{scr}}} \exp\left(\frac{a}{T_{c6}^{1/3}}\right) \text{ s}, \quad (17)$$

where n_p is the proton density, becomes comparable to the contraction time (i.e., the timescale for the change in central temperature if degeneracy is mild),

$$t_{\text{cont}} \equiv -\frac{R}{dR/dt} = 115 \left(\frac{3000 \text{ K}}{T_{\text{eff}}}\right)^4 \left(\frac{0.1 M_\odot}{M}\right) \left(\frac{0.6}{\mu_{\text{eff}}}\right)^3 \left(\frac{T_c}{3 \times 10^6}\right)^3 \text{ Myr}. \quad (18)$$

The above equation is valid regardless of the degree of degeneracy so long as the star is well described by an $n = 3/2$ polytrope. However, for rough estimates, one can put $\mu_{\text{eff}} = \mu \equiv (1/\mu_i + 1/\mu_e)^{-1}$

in equations (17) and (18). Evaluating $t_{\text{dest}} = t_{\text{cont}}$ at the stellar center gives an approximate condition for the central temperature at the time of depletion,

$$\frac{a}{T_c^{1/3}} = 32.9 + \ln(Sf_{\text{scr}}) - 3 \ln\left(\frac{M}{0.1M_\odot}\right) - 4 \ln\left(\frac{T_{\text{eff}}}{3000 \text{ K}}\right) - 6 \ln\left(\frac{\mu_{\text{eff}}}{0.6}\right) + (6 - j) \ln T_c. \quad (19)$$

The destruction time is a very steep function of the central temperature: once T_c reaches a certain value, the entire abundance of a light element is depleted on a timescale much shorter than t_{cont} . For example, a $0.1M_\odot$ star with $T_{\text{eff}} = 3000 \text{ K}$ burns ${}^7\text{Li}$ when the central temperature $T_c \approx 3 \times 10^6 \text{ K}$. Under these conditions, the reaction rate is extremely temperature sensitive ($N_A \langle \sigma v \rangle \propto T^{20}$) and the central temperature necessary for elemental depletion depends only weakly on mass. The sharp dependence of the reaction rate on the central temperature means that our calculations are extremely insensitive to small uncertainties in the constitutive physics, such as screening ($B^2\text{MU}$). For example, the central temperature at depletion is proportional to $(Sf_{\text{scr}})^{1/20}$ and the time of depletion $t \propto T_c^3 \propto (Sf_{\text{scr}})^{3/20}$. An uncertainty in the reaction rate or the screening correction by a factor of 2 can change the depletion time by no more than 10%. The exact equation for elemental depletion (which we derive below) is just a fancy way of writing $t_{\text{cont}} = t_{\text{dest}}$ that includes all the prefactors that arise from integrating the destruction rate over the entire star, and from the changing degeneracy (i.e., the decrease of μ_{eff}) during contraction.

At a given time t , consider a mass shell of coordinates $(m, m + dm)$ that contains $f(m, t) dm$ grams of a given light element isotope. There are two contributions to the rate of change of $f(m, t)$: (1) proton-capture reactions, and (2) convective transport from isotope-rich regions to isotope-poor regions. We ignore diffusion, as it occurs over timescales too long to be of any relevance. Symbolically,

$$\left(\frac{\partial f}{\partial t}\right)_m = \frac{fX\rho(m, t)}{m_H} \langle \sigma v \rangle(m, t) + \frac{\partial F}{\partial m}, \quad (20)$$

where F is the net mass of the light isotope transported per second by convection across a surface $r(m)$ at a time t , where m_H is the hydrogen mass. The term $\partial F/\partial m$ vanishes upon integration over the entire star. Defining the mass-averaged value of f by the equation $M\bar{f} \equiv \int_0^M f dm$, we integrate equation (20) over the star to obtain

$$M \frac{d\bar{f}}{dt} = - \int_0^M \frac{Xf}{m_H} \rho \langle \sigma v \rangle dm. \quad (21)$$

The timescale for a fluid element to traverse the radius is $t_{\text{mix}} \sim \ell/v$, where ℓ is the total length traveled. For a random walk process (Bodenheimer 1965), $\ell \sim R^2/\lambda_P$, where λ_P is the pressure scale height, which is of the order of the mixing length. The velocity may be estimated for the case of efficient convection, giving $t_{\text{mix}} \sim 10\text{--}100 \text{ yr}$ in the core. Inserting a value of ℓ appropriate for the photosphere gives $t_{\text{mix}} \sim 10^3 \text{ yr}$, which is still much shorter than the evolutionary time scale of $10^6\text{--}10^8 \text{ yr}$. Therefore, the star is well mixed and $f(m, t)$ can be replaced by $\bar{f}(t)$ in the integral. Then, upon changing variables to spatial coordinates in the RHS of equation (21), we have

$$\frac{d}{dt} \ln f = - \frac{4\pi X}{m_H M} \int_0^R \rho^2 \langle \sigma v \rangle r^2 dr. \quad (22)$$

For simplicity of notation, we drop the bar over f .

Using the non-resonant form of the reaction rate (eq. [15] with $j = 2/3$) and the definitions of central density and temperature (eqs. [5] and [6]), we write the differential equation describing the change of mass fraction f as

$$\frac{d}{dt} \ln f = -\frac{4\pi X}{\xi_1^3} \frac{\rho_c^2 R^3}{M} \frac{S}{N_A m_H} \left(\frac{\alpha}{a}\right)^2 \int_0^{\xi_1} f_{\text{scr}} \xi^2 \Theta^{7/3} \exp(-\alpha \Theta^{-1/3}) d\xi \quad s^{-1}, \quad (23)$$

where $\alpha \equiv aT_{c6}^{-1/3}$. The burning rate is very temperature-sensitive because the center of the star is much colder than the Gamow energy. This sensitivity restricts the burning to the central region of the star, where the temperature and density are quadratic in radius. Specifically, the peak of the rate integrand lies at $\xi_{\text{peak}} \approx 0.042 (55/\alpha)^2 + 0.0067 (55/\alpha)$. For this same reason we approximate the screening factor by its value at the center of the star. We then find an analytic approximation to the above equation that is accurate to within 1% for $\alpha > 45$ by using the first two terms of the expansion $\Theta(\xi) = 1 - \xi^2/6 + \dots$ and taking the upper limit to infinity. This yields:

$$\frac{d}{dt} \ln f = -0.18 \left(\frac{X}{0.7}\right) \left(\frac{0.6}{\mu_{\text{eff}}}\right)^3 \left(\frac{M_{\odot}}{M}\right)^2 S f_{\text{scr}} a^7 \alpha^{-17/2} \left(1 - \frac{21}{2\alpha}\right) e^{-\alpha} s^{-1}. \quad (24)$$

A similar development for resonant rates (with j kept as a parameter) yields

$$\frac{d}{dt} \ln f = -0.18 \left(\frac{X}{0.7}\right) \left(\frac{0.6}{\mu_{\text{eff}}}\right)^3 \left(\frac{M_{\odot}}{M}\right)^2 S f_{\text{scr}} a^{9-3j} \alpha^{-(21/2-3j)} \left(1 - \frac{27-9j}{2\alpha}\right) e^{-\alpha} s^{-1}. \quad (25)$$

In order to integrate this equation, we need to know the dependence of the central temperature parameter α on time, which is found by using the polytrope equation (6) and the degeneracy relation (eq. [10]):

$$\frac{\alpha}{a} = 0.513 \left(\frac{0.6}{\mu_{\text{eff}}}\right)^{1/3} \left(\frac{M_{\odot}}{M}\right)^{1/3} \left(\frac{R}{R_{\odot}}\right)^{1/3} = 6.73 \left(\frac{M}{M_{\odot}}\right)^{2/9} \left(\frac{\mu_e F_{1/2}(\eta)}{t_6 T_{e3}^4}\right)^{2/9}. \quad (26)$$

The value of $F_{1/2}(\eta)$ is obtained by solving the transcendental equation (10). Then we can use equation (26) to integrate the depletion equation (eq. [24] or eq. [25]) numerically from $t = 0$ and $\ln f = 0$ to find the element abundance as a function of time. Results of the calculations based on this formalism are presented in § 5.

In the region of the parameter space where degeneracy effects are not dominant (i.e., to the right of the constant degeneracy line (*heavy dotted line*) in Figure 1), the above derivation can be considerably simplified, and the depletion equation (either eq. [24] or [25]) can be integrated analytically (see B²MU for a simple version of this development). During contraction, the central temperature initially increases because the radius decreases (from the virial theorem for a nondegenerate ideal gas $T_c \propto M/R$). For a nondegenerate gas, $1/\mu_{\text{eff}} = 1/\mu_i + 1/\mu_e$, but when degeneracy becomes important μ_{eff} decreases, leading to a decrease in central temperature. Explicitly, we have

$$\frac{d}{dt} \ln f = \frac{d \ln f}{d\alpha} \frac{d\alpha}{dt} = \frac{d \ln f}{d\alpha} \left(\frac{\partial \alpha}{\partial R} \frac{dR}{dt} + \frac{\partial \alpha}{\partial \mu_{\text{eff}}} \frac{d\mu_{\text{eff}}}{dt} \right). \quad (27)$$

When degeneracy is not important (roughly, for $M \gtrsim 0.2M_\odot$), $\dot{\mu}_{\text{eff}}$ is negligible compared to \dot{R} . Thus, we can rewrite the depletion equation (25) in a simple form

$$\begin{aligned} \frac{d}{d\alpha} \ln f &= 6.23 \times 10^{14} \left(\frac{X}{0.7}\right) \left(\frac{0.6}{\mu_{\text{eff}}}\right)^6 \left(\frac{1000 \text{ K}}{T_{\text{eff}}}\right)^4 \left(\frac{M_\odot}{M}\right)^3 \\ &\times S f_{\text{scr}} a^{18-3j} \alpha^{-(41/2-3j)} e^{-\alpha} \left(1 - \frac{27-9j}{2\alpha}\right). \end{aligned} \quad (28)$$

This equation may be integrated directly from the initial condition $\alpha_0 = \infty$ to α :

$$W \equiv \ln \frac{f_0}{f} = 6.23 \times 10^{14} \left(\frac{X}{0.7}\right) \left(\frac{0.6}{\mu_{\text{eff}}}\right)^6 \left(\frac{1000 \text{ K}}{T_{\text{eff}}}\right)^4 \left(\frac{M_\odot}{M}\right)^3 S f_{\text{scr}} a^{18-3j} g(\alpha), \quad (29)$$

where

$$g(\alpha) = \left[\alpha^{-(41/2-3j)} e^{-\alpha} - \frac{68-15j}{2} \Gamma(-(41/2-3j), \alpha) \right] \quad (30)$$

and $\Gamma(x, \alpha)$ is the incomplete gamma function. For a given W , equation (29) can be solved for $\alpha(W)$, which is essentially the central temperature required for the level of depletion W . This is the method used in B²MU to compute ⁷Li depletion. We find that the two approaches (neglecting or including $\dot{\mu}_{\text{eff}}$) agree very well whenever the approximate formulation, equation (28), is valid.

We note that the treatment of degeneracy and screening in equation (29) is approximate in the following sense. In addition to neglecting $\partial\alpha/\partial\mu_{\text{eff}}$ when changing variables from t to α , we neglected the dependence of μ_{eff} and f_{scr} on α when integrating equation (28). This is justified because, when degeneracy is mild, μ_{eff} and f_{scr} vary very slowly with α , while the radius R is a strong function of α . Furthermore, the contraction rate of the star is $dR/dt \propto R^4$, so the star spends most of the time at smaller radii, where the contraction rate is small. Thus, to approximate electron degeneracy and screening corrections we just use the final values of $\mu_{\text{eff}}(\alpha, M)$ and $f_{\text{scr}}(\alpha, M)$ in equation (29) and solve the resulting transcendental equation. We find that the errors introduced by this approximation, as compared to integrating equations (24) or (25) directly are never more than a few percent. For rough estimates that neglect effects of degeneracy and screening, one can just set $1/\mu_{\text{eff}} = 1/\mu_i + 1/\mu_e \equiv 1/\mu$ and $f_{\text{scr}} = 1$.

5. Discussion of the Results for Each Light Element

We have presumed that the contracting pre-main-sequence star is well described as a fully convective $n = 3/2$ polytrope of arbitrary degeneracy with no substantial internal energy generation. This limits our light element depletion calculations in three ways:

1. **Onset of Hydrogen Burning.** Hydrogen burning begins (see § 2.2) before the star settles onto the zero-age main sequence and thereby increases the time needed for the star to reach a given radius, as compared to equation (9). Since we do not include this effect in our calculations, we limit our discussion to those stars generating less than 5% of their luminosity by hydrogen burning.

2. **Development of a Radiative Core.** Depletion at the stellar surface is directly related to the central temperature only when the star is fully convective. Further depletion will occur in the interior parts of the star, but the surface abundance of a light element is then sensitive to the temperature at the radiative/convective boundary and not to the central temperature. We stop calculating depletion when the core of the star becomes radiative (see § 2.2).
3. **Coulomb Effects on the Equation of State.** Depending on the particular element considered, Coulomb corrections to the equation of state can be important at the time of depletion. These act to break the polytropic nature of the star and increase the central temperature relative to the polytropic value (see § 5.1.1).

Figure 1 displays our results for central temperatures when the ${}^7\text{Li}$ abundance varies from a half to a hundredth of its initial value (*shaded region*). We also plot our central temperatures at one-half depletion of ${}^6\text{Li}$ (*light dotted line*) and ${}^9\text{Be}$ (*light dashed line*). (The boron isotopes are discussed in § 5.3.) The same curves, expressed in terms of mass and age, are shown in Figure 2 and motivate the following discussions for each element.

5.1. Lithium Depletion

The substantial amount of lithium² observations already makes the case that lithium abundances are a reliable indicator of stellar ages and masses (Rebolo, Martín, & Magazzù 1992; Martín et al. 1994; Basri et al. 1996; Rebolo et al. 1996; Oppenheimer et al. 1997). In § 5.1.2 we present an extended discussion of the observations of the cluster Alpha Persei and derive a minimum age of 60 Myr. Since this same technique can be applied to clusters in the age range of 10–200 Myr, we extensively discuss the application of our results to the lithium observations.

Previously (in B²MU), we discussed the lithium depletion results and provided convenient fitting formula. In addition to providing slightly improved formulae here, we also discuss in detail the limitations of our work at the very low-mass end. The intersection of the lithium depletion with the onset of a radiative core (see Figures 1 and 2) confines our work to $M \lesssim 0.46M_{\odot}$ (for this mass, the ending of convection in the core is concurrent with depletion of Li to 1% of its original abundance). Our method has the advantage of leaving T_{eff} independent of stellar mass, but the disadvantage of not including Coulomb effects, which limits us to masses $M \gtrsim 0.072 M_{\odot}$, or, for typical values of T_{eff} , to stars younger than $\sim 200 - 300$ Myr.

²Throughout this section references to lithium mean ${}^7\text{Li}$, as ${}^6\text{Li}$ always depletes first and is less abundant in the local ISM (Lemoine, Ferlet, & Vidal-Madjar 1995).

5.1.1. Comparison to Previous Theoretical Work and Limitations at Low Masses

Based on the results presented in B²MU, and using a fiducial effective temperature relation, $T_{\text{eff}} \propto M^{1/7}$, we obtain the central temperature at the time of one-half lithium depletion, $T_c \approx 3.1 \times 10^6 \text{ K} (M/0.1M_\odot)^{1/6}$. From the polytropic relation (eq. [5]), the central density at this time is $\rho_c \approx 62 \text{ g cm}^{-3} (0.1M_\odot/M)^{3/2}$. From T_c and ρ_c , we assess how important Coulomb corrections to the equation of state will be at the center of the star when the burning occurs. The plasma parameter at the time of one-half depletion is

$$\Gamma(1/2 \text{ } ^7\text{Li depletion}) \approx \frac{e^2}{k_B T} \left(\frac{4\pi\rho}{3m_H} \right)^{1/3} \approx 0.3 \left(\frac{0.1M_\odot}{M} \right)^{2/3}. \quad (31)$$

Accurate evaluations of the equation of state in this regime are known (see Saumon et al. 1996). However, we will roughly estimate the size of the Coulomb correction using the Coulomb pressure for $\Gamma \ll 1$ (Clayton 1983), $P_C = -e^3/3(\pi/k_B T)^{1/2}(1.8\rho/m_H)^{3/2}$, which then gives

$$\frac{P_C}{P} \approx -6.8 \times 10^{-2} \left(\frac{0.1M_\odot}{M} \right), \quad (32)$$

at the time of one-half depletion. Since the Coulomb pressure is negative, the central temperature is higher than its polytropic value.

Our neglect of the Coulomb correction places a lower limit on the mass of a star for which we can reliably compute the light element depletion. It is easy to show that, for normal composition ($X = 0.7$), the central temperature as a function of degeneracy is

$$T_c = 5.63 \times 10^6 \left(\frac{M}{0.075M_\odot} \right)^{4/3} \left(\mu_{\text{eff}} F_{1/2}^{1/3}(\eta) \right)^2 \text{ K}. \quad (33)$$

As the star contracts, the central temperature rises until the degree of degeneracy reaches a critical value ($F_{1/2}(\eta) \approx 4 - 6$), after which the central temperature begins to decline. The maximum value of T_c is

$$T_{c,\text{max}} = 3.43 \times 10^6 \left(\frac{M}{0.075M_\odot} \right)^{4/3} \text{ K}. \quad (34)$$

We note that equation (34) fully incorporates the effects of partial electron degeneracy, while a similar relation for $T_{c,\text{max}}$ using an approximate treatment of degeneracy is derived in Stevenson (1991) and Burrows & Liebert (1993). The maximum temperature as a function of mass (for $M < 0.1M_\odot$) is denoted with a thick dashed line in Figure 1. The intersection of this curve with the lithium depletion line defines the lower mass limit of validity of our lithium depletion calculations.

For high-mass stars that deplete lithium long before the central temperature reaches its peak, our neglect of Coulomb corrections slightly delays the time of depletion. This is because the Coulomb corrections allow the star to reach a given T_c at an earlier time and thereby deplete earlier. Roughly, since the time to reach a given central temperature scales as T_c^3 , we expect a 2%

error in the central temperature to give a 6% error in time. However, the stars that deplete lithium after (or while) contracting past the maximum temperature point always have $t_{\text{dest}} \gg t_{\text{cont}}$. Small corrections to the equation of state then have a large effect on the depletion time. Thus, our results are only reliable for stars that deplete lithium before reaching the maximum central temperature point, or that are younger than

$$t = 235 \left(\frac{M}{0.075 M_{\odot}} \right)^3 \left(\frac{2800 \text{ K}}{T_{\text{eff}}} \right)^4 \text{ Myr}, \quad (35)$$

which limits us to masses $M \gtrsim 0.072 M_{\odot}$ for lithium depletion by a factor of 100. The exact value of the low-mass cutoff is sensitive to the effective temperature, and Figure 3 displays the dependence of the cutoff mass on T_{eff} and the level of depletion. For a given level of depletion, our calculations are valid only to the right of the corresponding curve in Figure 3. For masses lower than the above cutoff, one needs to include all of the relevant corrections to the equation of state in order to reliably predict lithium depletion at low levels and we refer the reader to the papers of CB97 and DM94 for accurate calculations in this regime.

In order to simplify the use of our results in evaluating observations and comparing to detailed calculations, we have constructed simple analytic fits to the solutions of equations (24) and (25). The fits for age and central temperature of a star at a certain stage of ${}^7\text{Li}$ depletion (good for $0.072 M_{\odot} \lesssim M \lesssim 0.44 M_{\odot}$ for ${}^7\text{Li}$ depletion by a factor of 100; the exact range is outlined in Figures 1 and 3) are

$$\begin{aligned} t({}^7\text{Li}) &= 50.6 \left(\frac{0.1 M_{\odot}}{M} \right)^{0.707} \left(\frac{3000 \text{ K}}{T_{\text{eff}}} \right)^{3.516} \left(\frac{\mu_{\circ}}{\mu} \right)^{2.08} \left(\frac{W}{\ln 2} \right)^{0.121} \\ &\times \exp \left[0.0951 \left(\frac{0.1 M_{\odot}}{M} \right)^{5.02} \left(\frac{T_{\text{eff}}}{3000 \text{ K}} \right)^{0.599} \left(\frac{\mu_{\circ}}{\mu} \right)^{8.577} \left(\frac{W}{\ln 2} \right)^{0.148} \right] \text{ Myr} \end{aligned} \quad (36)$$

and

$$\begin{aligned} T_c({}^7\text{Li}) &= 3.06 \times 10^6 \left(\frac{M}{0.1 M_{\odot}} \right)^{0.149} \left(\frac{T_{\text{eff}}}{3000 \text{ K}} \right)^{0.158} \left(\frac{\mu}{\mu_{\circ}} \right)^{0.341} \left(\frac{W}{\ln 2} \right)^{0.039} \\ &\times \exp \left[-0.0149 \left(\frac{0.1 M_{\odot}}{M} \right)^{5.54} \left(\frac{T_{\text{eff}}}{3000 \text{ K}} \right)^{0.782} \left(\frac{\mu_{\circ}}{\mu} \right)^{9.37} \left(\frac{W}{\ln 2} \right)^{0.197} \right] \text{ K}, \end{aligned} \quad (37)$$

where $\mu_{\circ} = 4/(3 + 5X)$ for $X = 0.7$ and $W = \ln f_{\circ}/\ln f$. The accuracy of these fits (as well as all the other fits presented below) is better than 1% for the age and 0.3% for the central temperature. The corresponding fits for ${}^6\text{Li}$ are

$$\begin{aligned} t({}^6\text{Li}) &= 30.1 \left(\frac{0.1 M_{\odot}}{M} \right)^{0.72} \left(\frac{3000 \text{ K}}{T_{\text{eff}}} \right)^{3.532} \left(\frac{\mu_{\circ}}{\mu} \right)^{2.179} \left(\frac{W}{\ln 2} \right)^{0.117} \\ &\times \exp \left[0.0466 \left(\frac{0.1 M_{\odot}}{M} \right)^{5.088} \left(\frac{T_{\text{eff}}}{3000 \text{ K}} \right)^{0.575} \left(\frac{\mu_{\circ}}{\mu} \right)^{8.602} \left(\frac{W}{\ln 2} \right)^{0.142} \right] \text{ Myr} \end{aligned} \quad (38)$$

and

$$T_c({}^6\text{Li}) = 2.58 \times 10^6 \left(\frac{M}{0.1M_\odot}\right)^{0.144} \left(\frac{T_{\text{eff}}}{3000\text{K}}\right)^{0.15} \left(\frac{\mu}{\mu_\odot}\right)^{0.344} \left(\frac{W}{\ln 2}\right)^{0.037} \quad (39)$$

$$\times \exp \left[-0.006159 \left(\frac{0.1M_\odot}{M}\right)^{5.7} \left(\frac{T_{\text{eff}}}{3000\text{K}}\right)^{0.755} \left(\frac{\mu_\odot}{\mu}\right)^{9.55} \left(\frac{W}{\ln 2}\right)^{0.19} \right] \text{K}.$$

In the above equations the exponential factor accounts for the effects of degeneracy; for $M \geq 0.2 M_\odot$ it can be set to 1 without sacrificing the accuracy of the fit.

In our previous paper (B²MU), we compared our calculations for central temperature and age as functions of lithium depletion to those of CBP96. We found that the discrepancies between our results (using their effective temperatures) and theirs increased with the amount of lithium depletion. This difference has now been resolved. In the calculation of CBP96, the timestep did not scale with the rapidly decreasing lithium depletion timescale; as a result, when t_{dest} became much less than the Kelvin-Helmholtz timescale, the change in lithium abundance was no longer accurately computed. With the timestep adjusted to resolve t_{dest} , their code produces central temperatures (ages) consistent with ours to within 2% (10%) for $0.09 < (M/M_\odot) < 0.2$, and to within 3% (15%) for $0.2 < (M/M_\odot) < 0.35$ (Baraffe 1997). Remaining discrepancies are now of comparable size to the differences between our results and those of DM94 (using the effective temperatures of DM94), and give us renewed confidence in our semi-analytic calculations. We also note that, since the time of elemental depletion is rather sensitive to the effective temperature ($t \propto T_{\text{eff}}^{-3.5}$), the typical observational errors of $\sim 5\%$ in T_{eff} lead to an uncertainty of $\sim 15\%$ in the age determination. On the other hand, the corresponding central temperature is rather insensitive to the errors in T_{eff} (B²MU).

5.1.2. Comparison to Observations: Alpha Persei

As an example of how our depletion calculations allow us to place constraints on ages of young clusters (first carried out in the Pleiades by Basri et al. 1996 and B²MU) we apply our work to the recently reported non-detection of lithium in faint objects in the α Per open cluster (Zapatero Osorio et al. 1996). We use their observed luminosities to infer the minimum age of the cluster, independent from the uncertainties in the effective temperature scale. From this minimum age and the observed effective temperatures we constrain the stellar masses.

As described in B²MU, if lithium is undetected to some limit $W = \ln(f_\odot/f)$ in a star with $-3.50 < \log(L/L_\odot) < -2.32$ then the star must be older than

$$t_{\text{min}} = 54.7 \left(\frac{10^{-2.5}L_\odot}{L}\right)^{0.922} \left(\frac{\mu_\odot}{\mu}\right)^{2.52} \left(\frac{W}{\ln 2}\right)^{0.0769} \text{Myr}. \quad (40)$$

This minimum age does not depend on the effective temperature; rather, the minimum arises because electron-degeneracy pressure becomes important as low-mass stars contract (B²MU). Equation (40) therefore describes an absolute minimum age for a lithium depleted star in the proper

luminosity range, independent of the uncertainties in the effective temperature scale. It is the dimmest star with no lithium that sets the most restrictive bound on the minimum age. Applying equation (40) to AP 279³ ($\log(L/L_\odot) = -2.49 \pm 0.05$), we find that the cluster, if coeval, must be older than 61 ± 7 Myr, where the error comes from the uncertainty in the luminosity. The most recent age determination for this cluster from main-sequence turnoff by Meynet et al. (1993) gave 53 Myr for moderate convective overshoot, and the conventional turnoff age without convective overshoot is 51 Myr (Mermilliod 1981). As with lithium dating of young stars in the Pleiades (Basri et al. 1996), we find that the nuclear age determination using lithium observations is consistent with traditional upper main-sequence fitting only if convective overshoot plays a significant role in the evolution of massive stars. The minimum age derived above implies that α Per is likely to be older than what has been previously inferred from main-sequence turnoff, even with moderate convective overshoot, in agreement with the conclusion of Zapatero Osorio et al. (1996). However, because of the uncertainty in the luminosity of AP 279, and if we allow a range of a few Myr in the ages of individual cluster stars, we cannot rule out the possibility that the lithium nuclear age and the conventional main-sequence turnoff age are consistent. If dimmer lithium-depleted stars are found in α Per, this consistency will be harder to maintain (Basri 1998).

Lithium ages of α Per and Pleiades are sensitive to the luminosities of their dimmest lithium-depleted members, $t_{\text{Li}} \propto L^{-0.9}$ (eq. [40]), and, hence, to the assumed distance to the clusters. However, since the age determined from the main-sequence turnoff scales as $t_{\text{MS}} \propto L^{-0.6}$ (Meynet et al. 1993), the *difference* between t_{Li} and t_{MS} is a weak function of the assumed distance. For example, the Pleiades would need to be at least a factor of 2 more distant for the lithium age to coincide with the upper main-sequence age with no convective overshoot.

Given the inferred minimum age, we use the observed luminosity and lithium abundance to set a lower bound on each star’s mass. Combining equations (8) and (9) yields the mass of a star that has a certain luminosity and age,

$$\frac{M}{M_\odot} = 0.122 \left(\frac{L}{10^{-2.5} L_\odot} \right)^{3/4} \left(\frac{t}{100 \text{ Myr}} \right)^{1/2} \left(\frac{3000 \text{ K}}{T_{\text{eff}}} \right). \quad (41)$$

Substituting the value of the minimum age into this equation gives the minimum mass for each cluster member that is fully convective and has not yet arrived on the main sequence. We illustrate this technique in Figure 4 for the stars AP279, AP272, and AP284. The shaded regions for each star represent the allowed values of mass and age given their level of lithium depletion. If we presume that they are all of an age equal to or larger than our minimum estimate, then we find the following minimum masses: AP143, $0.30M_\odot$; AP 296, $0.25M_\odot$; AP284, $0.18M_\odot$; AP268, $0.11M_\odot$; AP 272, $0.12M_\odot$; AP279, $0.09M_\odot$; and AP J0323+4853⁴, $0.09M_\odot$. It is important to keep in mind

³The latest spectral type α Per member considered by Zapatero Osorio et al. (1996) is AP J0323+4853. However, it is slightly brighter ($\log(L/L_\odot) = -2.46 \pm 0.06$) than AP 279, and hence yields a less stringent minimum age.

⁴It has recently been reported (Martín & Zapatero Osorio 1997) that the rotation period of AP J0323+4853 is

that the minimum mass determination, unlike the minimum age determination, depends on the effective temperature scale used, and so is subject to systematic errors.

5.2. Beryllium Depletion

Since our calculations require the star to be contracting and fully convective, or below the nuclear burning and radiative core lines in Figure 1, it is clear that our theory for ${}^9\text{Be}$ (standard rate) applies to stars with masses in the range $0.1\text{--}0.3 M_\odot$. All of these objects clearly deplete beryllium prior to reaching the main sequence, and for this mass range the age of the star at a given level of depletion is

$$t({}^9\text{Be}) = 99.6 \left(\frac{0.1M_\odot}{M}\right)^{0.711} \left(\frac{3000\text{ K}}{T_{\text{eff}}}\right)^{3.555} \left(\frac{\mu_\odot}{\mu}\right)^{2.172} \left(\frac{W}{\ln 2}\right)^{0.111} \quad (42)$$

$$\times \exp \left[0.3365 \left(\frac{0.1M_\odot}{M}\right)^{3.60} \left(\frac{T_{\text{eff}}}{3000\text{ K}}\right)^{0.424} \left(\frac{\mu_\odot}{\mu}\right)^{6.582} \left(\frac{W}{\ln 2}\right)^{0.098} \right] \text{ Myr},$$

while the central temperature is

$$T_c({}^9\text{Be}) = 3.92 \times 10^6 \left(\frac{M}{0.1M_\odot}\right)^{0.129} \left(\frac{T_{\text{eff}}}{3000\text{ K}}\right)^{0.146} \left(\frac{\mu}{\mu_\odot}\right)^{0.313} \left(\frac{W}{\ln 2}\right)^{0.036} \quad (43)$$

$$\times \exp \left[-0.057261 \left(\frac{0.1M_\odot}{M}\right)^{3.408} \left(\frac{T_{\text{eff}}}{3000\text{ K}}\right)^{0.521} \left(\frac{\mu_\odot}{\mu}\right)^{6.228} \left(\frac{W}{\ln 2}\right)^{0.134} \right] \text{ K}.$$

Stars with $M \lesssim 0.1M_\odot$ deplete beryllium while approaching the main sequence or residing on it. For these objects, we refer the reader to the results of Nelson et al. (1993) and CB97. For masses $0.1M_\odot < M < 0.3M_\odot$, our central temperatures (ages) differ by no more than 2% (13%) from those of CB97. Our comparisons are for abundances of more than 0.5 of the initial abundance, on account of the aforementioned error in the calculations of CB97.

If the reaction ${}^9\text{Be}(p, \alpha){}^6\text{Li}$ does proceed via a sub-threshold resonance (see § 3), then parameterizing the cross section by the reduced width (see eq. [16]) implies that the age and central temperature at a given depletion level are

$$t({}^9\text{Be}) = 100.8 \left(\frac{0.1M_\odot}{M}\right)^{0.699} \left(\frac{3000\text{ K}}{T_{\text{eff}}}\right)^{3.547} \left(\frac{\mu_\odot}{\mu}\right)^{2.142} \left(\frac{W}{\ln 2}\right)^{0.113} \left(\frac{0.1}{\theta}\right)^{0.227} \quad (44)$$

$$\times \exp \left[0.3435 \left(\frac{0.1M_\odot}{M}\right)^{3.612} \left(\frac{T_{\text{eff}}}{3000\text{ K}}\right)^{0.46} \left(\frac{\mu_\odot}{\mu}\right)^{6.8} \left(\frac{W}{\ln 2}\right)^{0.105} \left(\frac{0.1}{\theta}\right)^{0.217} \right] \text{ Myr}$$

7.6 hr. Using the formula for the radius (eq. [9]), we estimate the breakup spin period ($P_b \approx 2\pi(R^3/GM)^{1/2}$) for the best guess at minimum age (61.2 Myr) and mass ($0.09M_\odot$) to be ≈ 0.13 hr. Rotation is therefore unlikely to cause any deviations of the depletion time from our estimates (e.g., by decreasing the central temperature).

and

$$T_c(^9\text{Be}) = 4.19 \times 10^6 \left(\frac{M}{0.1M_\odot}\right)^{0.129} \left(\frac{T_{\text{eff}}}{3000\text{K}}\right)^{0.149} \left(\frac{\mu}{\mu_\odot}\right)^{0.314} \left(\frac{W}{\ln 2}\right)^{0.037} \left(\frac{0.1}{\theta}\right)^{0.075} \quad (45)$$

$$\times \exp \left[-0.0653 \left(\frac{0.1M_\odot}{M}\right)^{3.101} \left(\frac{T_{\text{eff}}}{3000\text{K}}\right)^{0.542} \left(\frac{\mu_\odot}{\mu}\right)^{6.372} \left(\frac{W}{\ln 2}\right)^{0.132} \left(\frac{0.1}{\theta}\right)^{0.266} \right] \text{K}.$$

For example, a star of mass $0.2 M_\odot$ at half-depletion will be 22% younger if the resonance exists and $\theta = 0.3$.

5.3. Boron Depletion

Unlike lithium and beryllium, the higher Coulomb barrier of boron means that it is depleted when either hydrogen burning or radiative heat transport is important. In Figure 5, we show the central temperature at the time when one-half of ^{10}B (*thin solid line*) and ^{11}B (*thin dotted line*) are depleted, *assuming* that the stars are fully convective and not burning hydrogen. As one can see, this assumption holds only for a very narrow range of masses for ^{10}B , and does not hold for ^{11}B at all. Thus we can only make qualitative conclusions about boron depletion during pre-main-sequence contraction. Only Nelson et al. (1993) and CB97 have tabulated the boron depletion. Neither of these authors displayed results for the less abundant isotope ^{10}B . If the resonance were not present in the $p+^{10}\text{B}$ reaction (see § 3), then ^{10}B would deplete after ^{11}B and their boron results would have been in error. However, Figure 5 clearly shows that the resonance-corrected rate for this reaction is large enough so as to make it deplete before ^{11}B , in which case the aforementioned calculations are indeed valid.

Our approximations are, however, applicable to stars in a certain mass range that deplete boron on the main sequence. While on the main sequence, the central temperature of a star is essentially fixed. Moreover, stars with $M \lesssim 0.3M_\odot$ are fully convective on the main sequence. For such stars the formalism developed in § 4 is fully applicable, and, in particular, equations (24) and (25) with $\alpha = \text{const}$ imply that the abundances of ^{10}B and ^{11}B will decay exponentially, at rates determined by the star’s central density and temperature. Exponential decay of ^{11}B is consistent with its abundances at 1 and 10 Gyr in Table 2 of CB97; for stars of mass $0.085M_\odot \lesssim M \lesssim 0.13M_\odot$, this depletion happens on the main sequence before the Hubble time. Moreover, the depletion time scale is an extremely strong function of mass within this mass range.

It is clear that boron abundance in low-mass ($M \lesssim 0.13M_\odot$) main-sequence stars may provide a valuable constraint on their masses and ages, if boron can be observed. However, the strong dependence of depletion on the central temperature, as well as the high central density of these stars, necessitate sophisticated calculations like those of CB97 to accurately relate depletion time scales to stellar masses.

6. Conclusions

The ability of stars to burn lithium, beryllium, and boron prior to reaching the main sequence has been recognized for quite some time. However, the observations of such depletion are just now becoming accessible for pre-main-sequence stars in nearby clusters. This has motivated our semi-analytic work on light element depletion for low-mass ($M \lesssim 0.5M_{\odot}$) pre-main-sequence stars and the application of our results to observations of lithium-depleted stars. Lithium observations are proving to be an excellent age indicator in open clusters (see B²MU for a more extensive discussion) and our new minimum age determination for α Per (60 Myr) is in reasonable agreement with that found by upper main-sequence modeling with mild convective overshoot. However, if dimmer lithium-depleted stars are found in α Per, more overshoot may be necessary in order to reconcile the lithium nuclear age with the upper main-sequence turnoff one (Basri 1998). In addition, the difference between the nuclear and upper main-sequence turnoff ages is rather insensitive to the distance to the cluster. We encourage observers to map out the lithium depletion region for pre-main-sequence stars in clusters of ages 10–200 Myr. This will provide an important check on the mass dependence of convective overshoot in the massive stars near the turnoff in these clusters. The main results of this paper are the fitting formulae for the age and central temperature as a function of mass, effective temperature, composition, and depletion level for ${}^7\text{Li}$ (eq. [36] and [37]), ${}^6\text{Li}$ (eq. [38] and [39]), and ${}^9\text{Be}$ (eq. [42] and [43]). These relations are robust and useful for evaluating observations and for comparing to detailed numerical calculations. Moreover, our results allow using the observed T_{eff} directly, instead of first placing a star on a theoretical evolutionary track, as well as exploring the effects of the different observational T_{eff} scales.

Lithium dating of open clusters will most certainly help answer the question of how massive a star can become a white dwarf (WD). Ever since the white dwarf survey of young clusters of Romanishin & Angel (1980), there have been spectroscopic followups on the WD candidates (Reimers & Koester 1988). In addition to measuring the masses of the WD’s, the ultimate goal of these efforts is to learn the range of stellar masses that can become isolated WD’s. Crucial to this program is the ability to subtract the white dwarf cooling age from the cluster age so as to get the white dwarf birthday and thereby the mass of the progenitor star at that time. The most recent work of this nature is in NGC 2516 (Koester & Reimers 1993), which has an age inferred from the upper main-sequence turnoff of 140 Myr (Meynet et al. 1993), giving an inferred mass of the progenitor star of around $6 M_{\odot}$ (see also Reid 1996 for detailed discussion). Lithium dating of this (and other) young clusters would enhance our confidence in the extrapolation required to obtain the WD progenitor mass.

In the cold atmosphere of a low-mass star, the typically observed absorption lines of beryllium, 3130 and 3131Å, and boron, 2497 and 2498Å (Boesgaard 1996), lie in a part of the continuum where there are nearly no photons. Observations of pre-main-sequence depletion similar to those carried out for lithium thus await more sensitive instruments. There is, however, one intriguing possibility for diagnosing the elemental abundance of the surfaces of the low-mass main-sequence stars that might not have depleted beryllium or boron. Some of these low-mass objects are known to reside in

accreting binaries with white dwarfs, especially those with orbital periods below 2 hours (Warner 1995). Most of these binaries are dwarf novae, in which the matter leaving the low-mass star due to Roche lobe overflow accumulates in the disk for some time before reaching a thermal instability strong enough to dump the matter onto the white dwarf. There have been recent HST observations of the white dwarf photosphere after these accretion events (Sion 1995; Sion et al. 1997; Cheng et al. 1997) which show that the WD is heated by accretion. Since the matter at the photosphere is actually from the low-mass star, there may be a chance of seeing some features from the beryllium and boron that are now residing in the WD photosphere, where the continuum in the blue/UV is much higher. This approach is complicated by the fact that nearly all binary evolution calculations suggest that low-mass objects in systems with such short periods have experienced substantial mass transfer. This means that the progenitors of these low-mass stars are likely to have been more massive in the past, and may have depleted beryllium and boron in their cores.

We thank Gibor Basri, Lynne Hillenbrand, Eduardo Martín, and Maria Rosa Zapatero Osorio for keeping us up to date on the observational situation regarding lithium depletion and comments on the manuscript, Isabelle Baraffe for numerous comparisons with our results, Gerhard Raimann and Thomas Rauscher for communications about proton capture on boron, and the anonymous referee for his/her helpful comments. G. U. thanks the Fannie and John Hertz Foundation for fellowship support. C. D. M. was supported by an NSF Graduate Research Fellowship, and E. F. B. was supported by a NASA GSRP Graduate Fellowship under grant NGT-51662. L. B. acknowledges support as an Alfred P. Sloan Foundation fellow.

A. Fitting Formula for the Zero-Age Main Sequence

Using the formalism presented in § 2.2, we present a convenient fitting formula for the zero-age mainsequence (ZAMS) radius as a function of mass and effective temperature,

$$\frac{R}{R_{\odot}} = 0.129 \left(\frac{M}{0.1M_{\odot}} \right)^{0.766} \left(\frac{T_{\text{eff}}}{3000 \text{ K}} \right)^{-0.397} \exp \left[-0.192 \left(\frac{M}{0.1M_{\odot}} \right)^{-5.73} \left(\frac{T_{\text{eff}}}{3000 \text{ K}} \right)^{1.48} \right]. \quad (\text{A1})$$

This fit is good for $0.1 < M/M_{\odot} < 0.3$ and $2500 \text{ K} < T_{\text{eff}} < 3500 \text{ K}$. As a test of our approximations, we compare our radii to 1 Gyr isochrones from CB97 and DM94. We take the effective temperatures from the isochrone for each mass. Our radii deviate by no more than 2% ($0.15 < M/M_{\odot} < 0.3$) from Table 2 of CB97, and the maximum deviation for $0.1 < M/M_{\odot} < 0.3$ is 10%. The increasing deviation at lower masses is due to the Coulomb correction to the equation of state. From Figure 1, the 1 Gyr isochrone of CB97 lies slightly above the maximum temperature reachable with our approximations (i.e., with Coulomb effects neglected). Our radii deviate no more than 8% (7%) from those inferred from Table 5 (6) of DM94.

In Figure 6, we plot the surface gravity $\log g$ as a function of T_{eff} for $M/M_{\odot} = 0.12, 0.16, 0.20, 0.24,$ and 0.30 . Unfortunately, there is only one binary with stars in the mass range of our fit. This is the binary CM Draconis (Lacy 1977), which has a primary (secondary) of mass $(0.237 \pm 0.011)M_{\odot}$ [$(0.207 \pm 0.008)M_{\odot}$] and effective temperature of $(3150 \pm 100) \text{ K}$ (same for the secondary). Using these parameters, we infer a radius of $0.246R_{\odot}$ ($0.221R_{\odot}$) and a surface gravity $\log g = 5.03$ ($\log g = 5.07$); the values from Lacy (1977) are $(0.252 \pm 0.008)R_{\odot}$ [$(0.235 \pm 0.007)R_{\odot}$] and 5.01 ± 0.05 (same for the secondary).

Similar fits were recently presented by Tout et al. (1996) for the ZAMS radii as functions of mass and metallicity. Our fits have the advantage of being in terms of mass and effective temperature, and so are independent of the model assumptions that are incorporated in mapping the metallicity to the effective temperature.

Table 1. Proton Capture Rate Parameters

Reaction	S	a	j	References
${}^6\text{Li}(p, {}^3\text{He}) {}^4\text{He}$	3.75×10^{12}	84.13	2/3	1
${}^7\text{Li}(p, \alpha) {}^4\text{He}$	7.20×10^{10}	84.72	2/3	1,2
${}^9\text{Be} + p$ (nonresonant)*	$2 \times 2.18 \times 10^{13}$	103.59	2/3	1
${}^9\text{Be}(p, \alpha) {}^6\text{Li}$ (resonant)	$3.53 \times 10^{16}\theta^2$	105.33	1.367	3
${}^{10}\text{B}(p, \alpha) {}^7\text{Be}$	2.18×10^{15}	120.62	1/6	1,2
${}^{11}\text{B}(p, \alpha) 2 {}^4\text{He}$	2.22×10^{14}	120.95	2/3	1,4

*Includes contributions from ${}^9\text{Be}(p, {}^2\text{H}) 2 {}^4\text{He}$ and nonresonant ${}^9\text{Be}(p, \alpha) {}^6\text{Li}$ rates.

References. — (1) CF88; (2) Raimann 1993; (3) Brown 1997; (4) Rauscher & Raimann 1996

REFERENCES

- Ajzenberg-Selove, F. 1988, Nucl. Phys. A, A490, 1
- Alexander, D.R., Augason, G.C., & Johnson, H.R. 1989, ApJ, 345, 1014
- Alexander, D.R., & Fergusson, J.W. 1994, ApJ, 437, 879
- Allard, F., & Hauschildt, P.H. 1997, in preparation
- Baraffe, I. 1997, private communication
- Basri, G., Marcy, G. W., & Graham, J. R. 1996, ApJ, 458, 600
- Basri, G. 1998, in Cool Stars in Clusters and Associations: Magnetic Activity and Age Indicators, Mem.S.A.It., ed. G. Micela, S. Sciortino, & R. Pallavicini, in press
- Bildsten, L., Brown, E. F., Matzner, C. D., & Ushomirsky, G. 1997, ApJ, 482, 442 (B²MU)
- Bodenheimer, P. 1965, ApJ, 142, 451
- Bodenheimer, P. 1966, ApJ, 144, 103
- Boesgaard, A.M. 1996, in Formation of the Galactic Halo...Inside and Out, ASP Conf. Ser., Vol. 92, ed. H. Morrison & A. Sarajedini (San Francisco: Freeman), 327
- Brown, E. F. 1997, ApJ, in press
- Burrows, A., Hubbard, W. B., & Lunine, J. I. 1989, ApJ, 345, 939
- Burrows, A., & Liebert, J. 1993, Rev. Mod. Phys., 65, 301
- Caughlan, G. R., & Fowler, W. A. 1988, Atomic Data and Nuclear Data Tables, 40, 283 (CF88)
- Chabrier, G., Baraffe, I., & Plez, B. 1996, ApJ, 459, L91 (CBP96)
- Chabrier, G., & Baraffe, I. 1997, A&A, 327, 1029 (CB97)
- Cheng, F. H., Sion, E. M., Szkody, P., & Huang, M. 1997, ApJ, 484, L149
- Clayton, D. D. 1983, Principles of Stellar Evolution and Nucleosynthesis (Chicago: Univ. of Chicago Press)
- D'Antona, F., & Mazzitelli, I. 1984, A&A, 138, 431
- D'Antona, F., & Mazzitelli, I. 1985, ApJ, 296, 502
- D'Antona, F., & Mazzitelli, I. 1994, ApJS, 90, 467 (DM94)
- Deliyannis, C. P., Demarque, P., & Kawaler, S. D. 1990, ApJS, 73, 21

- Ezer, D., & Cameron, A. G. W. 1963, *Icarus*, 1, 422
- Federman, S. R., Lambert, D. L., Cardelli, J. A., & Sheffer, Y. 1996, *Nature*, 381, 764
- Forestini, M. 1994, *A&A*, 285, 473
- Grossman, A. S., & Graboske, H. C. 1971, *ApJ*, 164, 475
- Grossman, A. S., & Graboske, H. C. 1973, *ApJ*, 180, 195
- Hansen, C. J., & Kawaler, S. D. 1994, *Stellar Interiors: physical principles, structure, and evolution* (New York: Springer-Verlag)
- Hayashi, C., & Nakano, T. 1963, *Prog. Theor. Phys.*, 30, 460
- Kirkpatrick, J. D., Kelly, D. M., Rieke, G. H., Liebert, J., Allard, F., & Wehrse, R. 1993, *ApJ*, 402, 643
- Koester, D., & Reimers, D. 1996, *A&A*, 313, 810
- Kurucz, R.L. 1991, in *Stellar Atmospheres: Beyond the Classical Models*, ed. L. Crivellari, I. Hubeny, & D.G. Hummer (NATO ASI Ser.; Dordrecht: Kluver), 441
- Lacy, C. H. 1977, *ApJ*, 218, 444
- Larson, R. B., & Demarque, P. R. 1964, *ApJ*, 140, 524
- Lemoine, M., Ferlet, R., & Vidal-Madjar, A. 1995, *A&A*, 298, 879
- Maeder, A., & Meynet, G. 1989, *A&A*, 210, 155
- Magazzù, A., Martín, E. L., & Rebolo, R. 1993, *ApJ*, 404, L17
- Martín, E. L. 1998, in *Cool Stars in Clusters and Associations: Magnetic Activity and Age Indicators*, *Mem.S.A.It.*, ed. G. Micela, S. Sciortino, & R. Pallavicini, in press
- Martín, E. L., & Claret, A. 1996, *A&A*, 306, 408
- Martín, E. L., Rebolo, R., & Magazzù, A. 1994, *ApJ*, 436, 262
- Martín, E. L., & Zapatero Osorio, M. R. 1997, *MNRAS*, 286, L17
- Mermilliod, J.-C. 1981, *A&A*, 97, 235
- Meynet, G., Mermilliod, J.-C., & Maeder, A. 1993, *A&AS*, 98, 477
- Nelson, L. A., Rappaport, S., & Chiang, E. 1993, *ApJ*, 413, 364
- Nelson, L. A., Rappaport, S. A., & Joss, P. C. 1986, *ApJ*, 311, 226

- Oppenheimer, B. R., Basri, G., Nakajima, T., & Kulkarni, S. R. 1997, *AJ*, 113, 296
- Piskunov, N., Wood, B.E., Linsky, J.L., Dempsey, R.C., & Ayres, T.R. 1997, *ApJ*, 474, 315
- Pozio, F. 1991, *Mem. Soc. Astron. Ital.*, 62, 171
- Proffitt, C. R., & Michaud, G. 1989, *ApJ*, 346, 976
- Raimann, G. 1993, *Z. Phys. A.*, 347, 73
- Rauscher, T., & Raimann, G. 1996, *Phys. Rev. C*, 53, 2496
- Rebolo, R., Martín, E. L., & Magazzù, A. 1992, *ApJ*, 389, L83
- Rebolo, R., Martín, E. L., Basri, G., Marcy, G. W., & Zapatero Osorio, M. R. 1996, *ApJ*, 469, L53.
- Reid, I. N. 1996, *AJ*, 111, 2000
- Reimers, D., & Koester, D. 1988, *ESO Messenger*, 54, 47
- Rogers, F. J., & Iglesias, C. A. 1992, *ApJS*, 79, 507
- Romanishin, W., & Angel, J. R. P. 1980, *ApJ*, 235, 992
- Salpeter, E. E., & Van Horn, H. M. 1969, *ApJ*, 155, 183
- Saumon, D., Chabrier, G., & Van Horn, H. M. 1995, *ApJS*, 99, 713
- Sion, E. M. 1995, in “White Dwarfs”, ed. D. Koester & K. Werner (Springer: Berlin), p. 208
- Sion, E. M., Cheng, F. H., Sparks, W. M., Szkody, P., Huang, M., & Hubeny, I. 1997, *ApJ*, 480, L17
- Soderblom, D. R. 1995, *Mem. Soc. Astron. Ital.*, 66, 347
- Stahler, S. W. 1988a, *ApJ*, 332, 804
- Stahler, S. W. 1988b, *PASP*, 100, 1474
- Stevenson, D. 1991, *ARA&A*, 29, 163
- Swenson, F. J., Stringfellow, G. S., & Faulkner, J. 1990, *ApJ*, 348, L33
- Swenson, F. J., Faulkner, J., Rogers, F. J., & Iglesias, C. A. 1994, *ApJ*, 425, 286
- Tout, C. A., Pols, O. R., Eggleton, P. P., & Han, Z. 1996, *MNRAS*, 281, 257
- Vandenberg, D. A., & Poll, H. E. 1989, *AJ*, 98, 1451
- Vauclair, S., Vauclair, G., Schatzman, E., & Michaud, G. 1978, *ApJ*, 223, 567

Warner, B. 1995, *Cataclysmic Variable Stars* (Cambridge: Cambridge Univ. Press)

Weymann, R., & Moore, E. 1963, *ApJ*, 137, 552

Zapatero Osorio, M. R., Rebolo, R. Martín, E. L., & García López, R. J. 1996, *A&A*, 305, 519

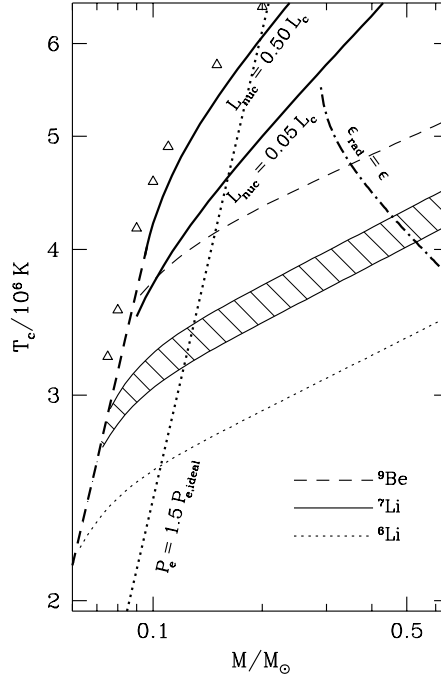


Fig. 1.— Constraints on validity of ${}^7\text{Li}$, ${}^6\text{Li}$, and ${}^9\text{Be}$ calculations. For ${}^7\text{Li}$ we show the temperatures at which the abundance falls from one-half to one-hundredth its initial value (*shaded region*). For ${}^6\text{Li}$ (*dotted line*) and ${}^9\text{Be}$ (*dashed line*) we plot only the curves along which one half of the element has been depleted. We also show the constraints on applicability of our depletion calculations. Stars above the line $\epsilon_{\text{rad}} = \epsilon$ (*heavy dot-dashed line*) have radiative cores, while the curves $L_{\text{nuc}} = 0.05 L_c$ and $0.50 L_c$ (*heavy solid lines*) herald the arrival of the star on the main sequence. For comparison, we show (*triangles*) central temperatures of young (1 Gyr) main-sequence stars (CB97, Table 2). Coulomb corrections are unimportant *except* where the central temperature is near the maximum set by degeneracy (*heavy dashed line*), as described in § 5.1.1. The maximum temperature curve is essentially a curve of constant degeneracy, as evidenced by the comparison with the curve where the electron pressure is 1.5 times its classical value (*heavy dotted line*).

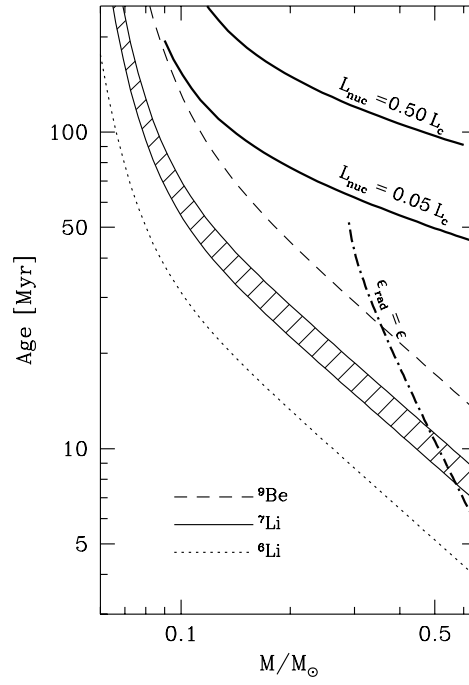


Fig. 2.— Same as Figure 1, but for stellar age instead of central temperature. The main sequence, the maximum central temperature, and the constant degeneracy lines are not shown. The effective temperature scale $T_{\text{eff}}(M)$ is from the results of Chabrier & Baraffe 1997.

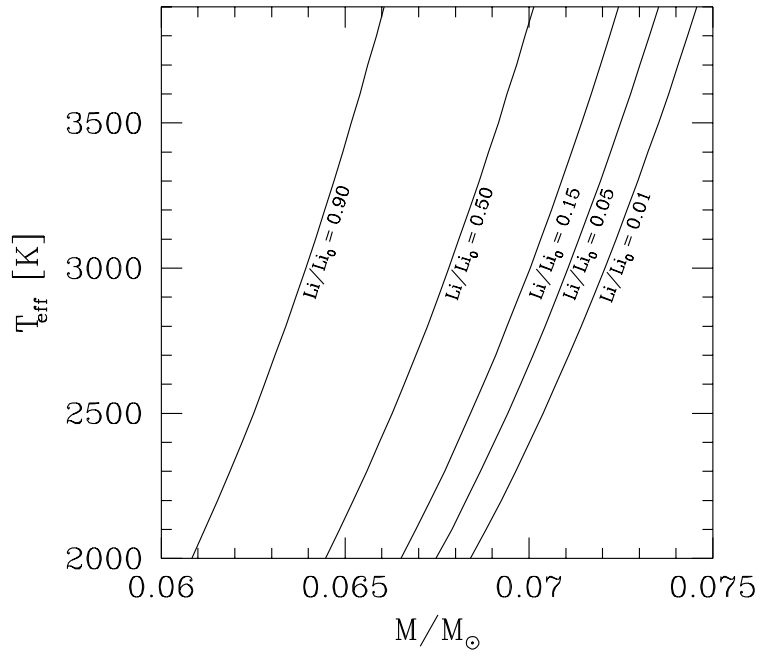


Fig. 3.— Minimum mass, as a function of effective temperature, for which our ${}^7\text{Li}$ depletion calculations are reliable. At a given effective temperature, we show the mass for which contraction at that T_{eff} implies that lithium is depleted to the given amount (${}^7\text{Li}/{}^7\text{Li}_0 = 0.01, 0.05, 0.15, 0.5,$ and 0.9) before the star reaches the maximum temperature set by degeneracy (eq. [34]).

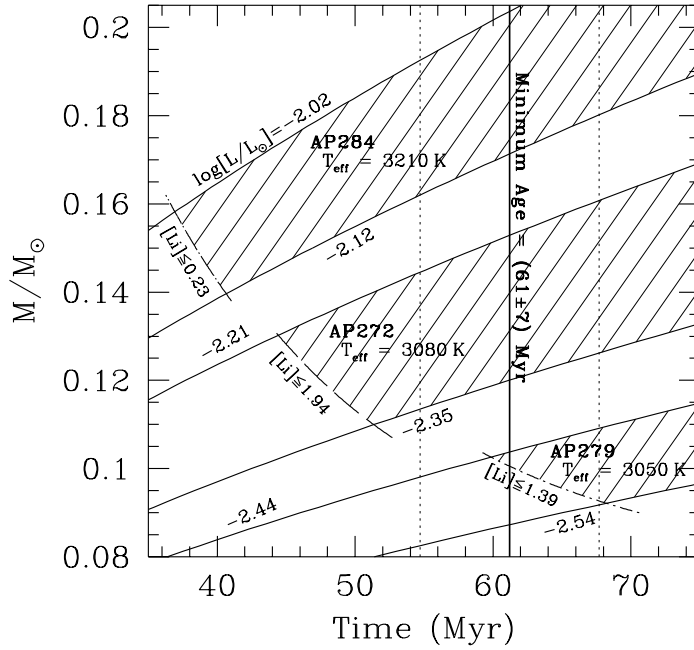


Fig. 4.— An illustration of how the minimum age derived from equation (40) may be used in conjunction with the mass-age relationship, equation (41), to set a lower bound on the masses of AP284, AP272, and AP279. We show the minimum cluster age (*heavy vertical solid line*) and its uncertainty (*light vertical dotted lines*). For each star, we plot two constant luminosity contours that correspond to the observational uncertainty in luminosity (*light solid lines*) and a contour of constant lithium abundance: AP284, $[\text{Li}] \equiv 12 + \log(N_{\text{Li}}/N_{\text{H}}) \leq 0.23$ (*dot-long dashed line*); AP272, $[\text{Li}] \leq 1.94$ (*dashed line*); and AP279, $[\text{Li}] \leq 1.39$ (*dot-short dashed line*). These constraints fence each star into a region of M - t space (*shaded areas*). The intersection of the shaded region with the minimum age curve sets a lower bound for the mass of each star.

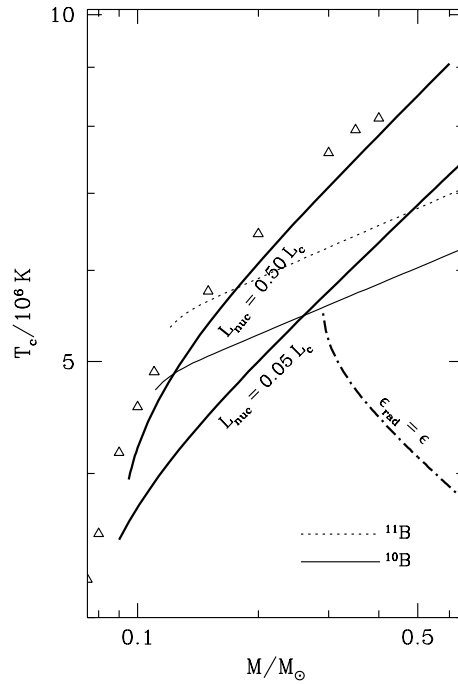


Fig. 5.— The central temperatures at which the abundances of ^{10}B (*light solid line*) and ^{11}B (*light dotted line*) have decreased to one-half their initial values, *presuming* that the star is fully convective and the p-p energy generation is negligible. We also indicate (*thick solid lines*) where nuclear reactions contribute 5% and 50% of the stellar luminosity, and also (*thick dot-dashed line*) where a radiative region develops in the core. For comparison, we display (*triangles*) a 1 Gyr isochrone from Table 2 of Chabrier & Baraffe (1997). Clearly, any treatment of boron depletion must include hydrogen burning. For a small range of masses about $0.1M_{\odot}$, boron depletion occurs on the main sequence.

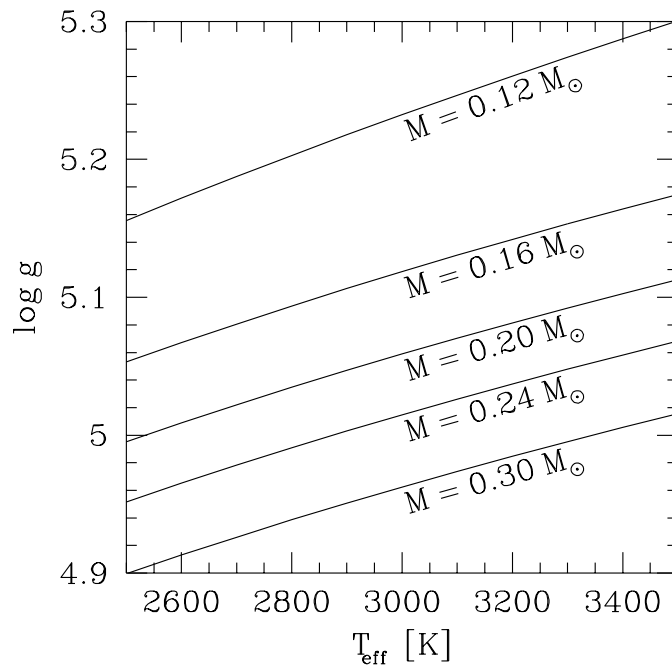


Fig. 6.— Each line is the $\log g$ – T_{eff} relation for a low-mass star (of mass indicated on the plot) on the Zero-Age Main Sequence (ZAMS). We calculate the ZAMS using the method outlined in section 2.2.